DOI: 10.1002/cmdc.201200566

[^{3}H]UR-PLN196: A Selective Nonpeptide Radioligand and Insurmountable Antagonist for the Neuropeptide Y Y_2 Receptor

Nikola Pluym, Paul Baumeister, Max Keller, Günther Bernhardt, and Armin Buschauer*[a]

Neuropeptide Y (NPY) has been reported to be involved in the regulation of numerous physiological processes and implicated in diseases such as obesity, depression and alcoholism (for recent Review articles, see. Ref. [1,2]). In humans, the biological effects of NPY are mediated by four functionally expressed receptor subtypes, designated Y_1, Y_2, Y_4 and Y_5 receptors (Y_1R, Y_2R, Y_4R, Y_5R). Numerous potent and selective Y_1R and Y_5R antagonists have been described since 1994, especially aiming at new drugs for the treatment of obesity. Argininamide BIIE 0246[3] (Scheme 1), the first reported potent and selective Y_2R antagonist, proved to be a valuable tool for the study of Y_2R. Meanwhile, there is growing interest in the Y_2R as a therapeutic target, not least stimulated by recently published brain-penetrant, orally available Y_2R antagonists such as JNJ-31020028,[4] JNJ-5207787[5] and SF-11[6] (Scheme 1), as well as structural analogues of the latter, such as CYM 9552 or CYM 9484,[7] and imidazolidine-2,4-diones, such as NVP-833.[8]

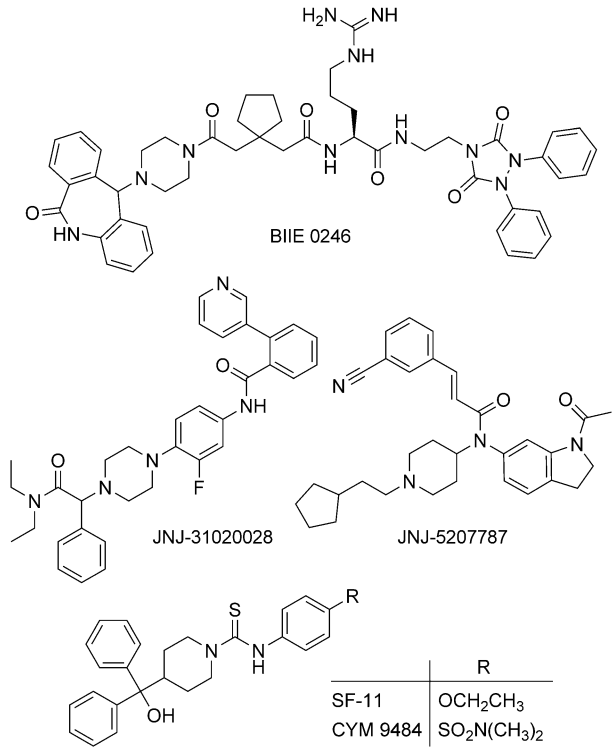

Scheme 1. Structures of nonpeptidic NPY Y_2 receptor antagonists.

Radioligands used for the study of Y_2R are, for instance, [^{3}H]NPY,[9,10] [^{125}I]PYY,[11] and [^{125}I]PYY(3–36),[12,13] which are devoid of subtype selectivity. Selective nonpeptidic radioligands for Y_2R are not available. Aiming at potent and subtype-selective tracers for Y_2R, we synthesized a series of derivatives of argininamide-type Y_2R antagonist BIIE 0246.[3] Previously, electron-withdrawing substituents, such as acyl and carbamoyl residues, attached to the guanidine group (N^G) of the parent compound were found to be tolerated despite the decrease in basicity by four to five orders of magnitude.[14] Derivatives bearing a terminal amino group (N^ω) in the acyl moiety are of special interest with respect to labeling with fluorescent dyes or radioisotopes. Starting from these precursors, we synthesized a small library of potential radioligands ("cold" forms) by propionylation of the terminal amino moiety with respect to selection of an appropriate candidate for radiolabeling.

N^G-Substituted amine precursors **11**–**20** were obtained by guanidinylation of the corresponding ornithinamide with differently substituted *N*-acyl-*N'*-*tert*-butoxycarbonyl-*S*-methylisothioureas **1**–**10** (Scheme 2), followed by acidic *tert*-butoxycarbonyl (Boc) deprotection (Scheme 3). Guanidinylating reagents **1**–**10** (for **5**, **6**, **8**, **10**, see Ref. [14]) were prepared by coupling the mono-Boc-protected *S*-methylisothiourea with the corresponding carboxylic acids (Scheme 2), which were either activated in situ with hydroxybenzotriazole (HOBt)/*N*,*N*,*N'*,*N'*-tetramethyl-O-(benzotriazol-1-yl)uronium tetrafluoroborate (TBTU) or used as commercially available succinimidyl esters (**2**–**4**, **6**). In the final reaction step, amine precursors **11**–**20** were acylated with succinimidyl propionate to yield Y_2R antagonists **21a** and **22**–**30** (Scheme 3). Mono-Boc-protected argininamide **33** was synthesized by guanidinylation with di-Boc-protected *S*-methylisothiourea followed by acidic cleavage of only one Boc group. Deprotection under acidic conditions using mixtures of acetonitrile and water containing 0.1% trifluoroacetic acid (TFA) was complete after three hours (monitored by HPLC). By analogy with the previously described synthesis of a N^G-propionylated argininamide-type Y_1R antagonist,[15] N^G-propionylated derivative **34** was obtained by acylation of **33** with **31a** and Boc deprotection (Scheme 3).

Amine precursors **11**–**20** (for **12**, **16**, **17**, **20**, see Ref. [14]) as well as propionamides **21a**, **22**–**30** and **34** were investigated for Y_2R binding and antagonism (Table 1). The Y_2R binding af-

[a] *Dr. N. Pluym, P. Baumeister, Dr. M. Keller, Prof. Dr. G. Bernhardt, Prof. Dr. A. Buschauer*
Institut für Pharmazie, Pharmazeutische/Medizinische Chemie
Universität Regensburg
Universitätsstr. 31, 93053 Regensburg (Germany)
E-mail: armin.buschauer@chemie.uni-regensburg.de

Supporting information for this article is available on the WWW under http://dx.doi.org/10.1002/cmdc.201200566.

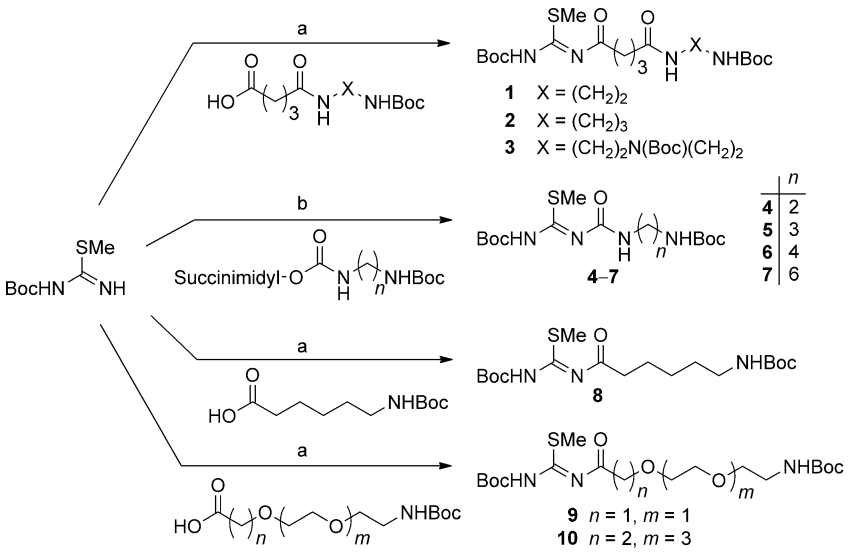

Scheme 2. Preparation of guanidinylating reagents **1**–**10**. *Reagents and conditions*: a) HOBt (1 equiv), TBTU (1 equiv), DIPEA (2 equiv), DMF, 16 h, RT; b) DIPEA (2 equiv), DMF, 16 h, RT.

All synthesized propionic amides exhibited a decreased affinity compared to the corresponding amine precursors, except for compound **23**, which contains an additional amine function in the linker that is positively charged at physiological pH. Apparently, an additional polar group in the acyl linker of the antagonists is preferred by Y_2R. "Masking" the positive charge by acylation with propionic acid resulted in a decrease in affinity, especially in the case of N^G-carbamoylated analogues **25**–**28**. Nevertheless, most of the synthesized potential radioligands possess Y_2R affinities in the one- to two-digit nanomolar range, for instance, **21a**, **23** and **24** (K_i values around 10 nM). Propionylation of BIIE 0246 in N^G-position yielded **34**, the compound with the highest Y_2R antagonistic activity (Table 1).

finities were determined in a flow cytometric binding assay, using CHO cells stably expressing the human Y_2 receptor (hY_2R),[16] and fluorescence-labeled pNPY (Cy5-pNPY or Dy-635-pNPY).[17] NPY Y_2R antagonistic activities were determined in a spectrofluorimetric Ca^{2+} assay (fura-2 assay) in CHO cells stably expressing hY_2R.[18]

Taking into consideration Y_2R affinity, synthetic pathway and overall yield, amine precursor **11** was selected for labeling. N^{ω}-[2,3-^{3}H]Propionyl-substituted argininamide **21b** ([^{3}H]UR-PLN196), the "hot" form of **21a**, was prepared by acylation

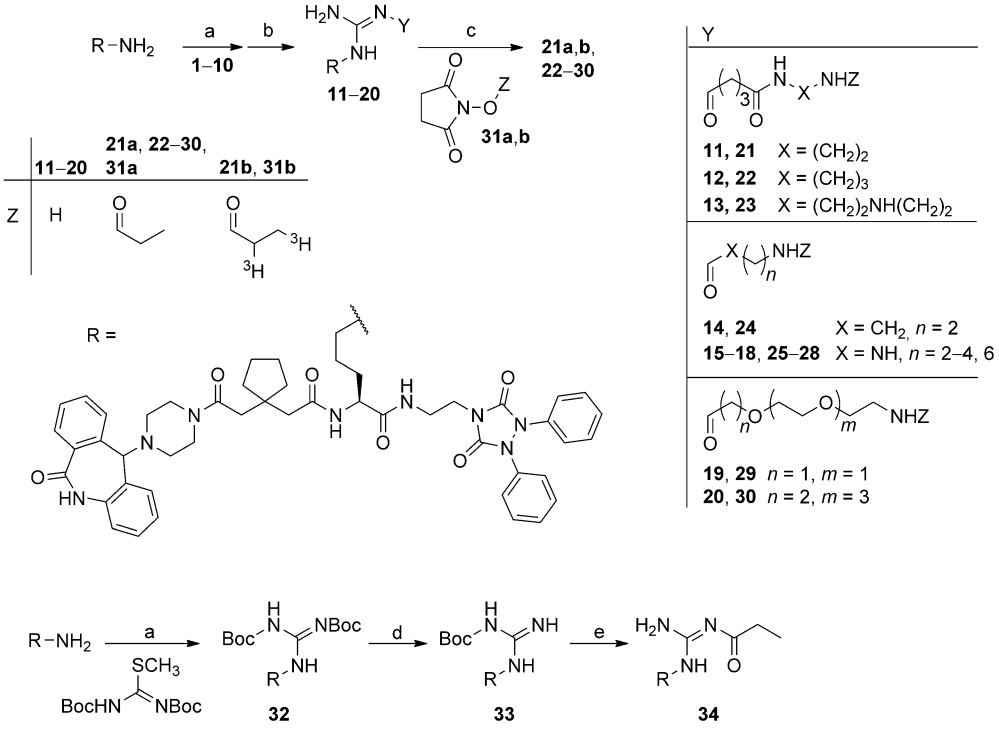

Scheme 3. Synthesis of N^G-substituted amine precursors **11**–**20**, corresponding potential radioligands **21a**, **22**–**30**, **34**, and tritiated ligand **21b**. *Reagents and conditions*: a) $HgCl_2$ (1 equiv), NEt_3 (2 equiv), DMF, 16 h, RT; b) TFA/CH_2Cl_2 (1:1 *v/v*), 2 h, RT; c) for **21a**, **22**–**30**: **31a** (1 equiv), NEt_3 (2 equiv), CH_3CN, 16 h, RT; for **21b**: **31b** (0.025 equiv), NEt_3 (2 equiv), CH_3CN, 20 h, RT; d) CH_3CN/0.1% aq. TFA (1:1 *v/v*), 5 h, RT; e) 1. **31a** (1.2 equiv), NEt_3 (1 equiv), CH_3CN, 21 h, RT; 2. TFA, 2 h, RT.

Table 1. Pharmacological data for Y_2R antagonistic amine precursors **11**–**20** and propionic amides **21 a**, **22**–**30**, **34**.

Compd	Linker length[a]	K_b[b] [nM]	K_i[c] [nM]
11	8	3.7 ± 0.1	3.4 ± 0.1
12[d]	9	4.4 ± 0.5	2.3 ± 1.4
13	11	16 ± 2	16 ± 3
14	6	1.0 ± 0.2	7.8 ± 1.0
15	4	7.0 ± 5.1	7.6 ± 4.2
16[d]	5	2.5 ± 0.2	2.1 ± 0.3
17[d]	6	1.8 ± 0.2	3.2 ± 0.3
18	8	2.1 ± 0.4	7.0 ± 1.2
19	8	6.5 ± 0.02	18 ± 1
20[d]	15	6.0 ± 0.5	8.1 ± 3.2
21 a	8	16 ± 8	9.9 ± 1.0[e]
22	9	8.5 ± 0.1	22 ± 6
23	11	16 ± 8	9.9 ± 1.1
24	6	11 ± 4	9.0 ± 0.2[e]
25	4	30 ± 11	64 ± 4
26	5	22 ± 2	32 ± 0.1
27	6	9.4 ± 0.1	55 ± 15
28	8	12 ± 5	84 ± 64
29	8	16 ± 2	15 ± 0.2
30	15	50 ± 3	48 ± 14
34	–	8.2 ± 0.4	5.2 ± 1.8

[a] Length of the linker expressed as the number of atoms connecting the argininamide N^G and the ω-amino function (for structures, see Scheme 3) [b] Inhibition of pNPY (70 nM)-induced $[Ca^{2+}]_i$ mobilization in hY_2R-expressing CHO cells; data represent the mean ± SEM (n = 2–5). [c] K_i values were determined in a flow cytometric binding assay from the displacement of Cy5-pNPY (K_d = 5.2 nM, c = 5 nM) on CHO-hY_2R cells, unless otherwise indicated; data represent the mean ± SEM (n = 2–4).[d] Data are in good agreement with those reported in Ref. [14], [e] Dy-635-pNPY was used as the fluorescent ligand (10 nM) for competition binding.

with commercially available tritiated succinimidyl propionate **31 b** (Scheme 2). After purification by HPLC, radioligand **21 b** was obtained in a radiochemical purity of > 99% (Figure 1) with a specific activity of (a_s) 80.7 Ci mmol^{-1}. The identity of the radioligand was confirmed by HPLC analysis of labeled

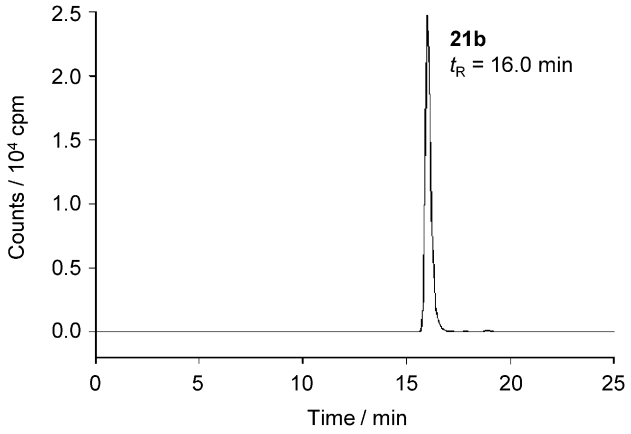

Figure 1. HPLC analysis (radiochromatogram) of [^{3}H]UR-PLN196 (**21 b**). Eluent: mixtures of CH_3CN + 0.05% TFA (A) and 0.05% aq. TFA (B), gradient: 0→20 min: A/B 30:70→60:40, 20→22 min: 60:40→95:5, 22→25 min: 95:5. The identity of **21 b** was confirmed by spiking with "cold form" **21 a** (UV detection; spectrum not shown).

(**21 b**) and unlabeled (**21 a**) UR-PLN196. Moreover, chemical stability in ethanol containing 100 μM TFA at −20 °C was proven over a period of at least 12 months (see the Supporting Information).

The selectivity of the BIIE0246 derivatives for human Y_2 over Y_1, Y_4, and Y_5 receptors was proven by flow cytometric binding assays using fluorescence-labeled pNPY (Y_1R, Y_5R) or [K^4]hPP (Y_4R) according to previously described methods (see Table 2 for selectivity data of **21 a**, the "cold" form of radioligand **21 b**).[17,19]

Table 2. NPY receptor subtype selectivity of **21 a**/**21 b**.

hY_2R K_d [nM]	hY_1R K_i [nM]	hY_4R K_i [nM]	hY_5R K_i [nM]
43[a] 67[b]	> 5000[c]	> 6500[c]	> 5000[c]

[a] Kinetically determined dissociation constant. [b] K_d from saturation binding. [c] Flow cytometric binding assays using 10 nM Cy5-pNPY (Y_1R), 5 nM Cy5-pNPY (Y_5R) or 3 nM Cy5-[K^4]-hPP (Y_4R) on HEL-Y_1, CHO-Y_4, and HEC-1B-Y_5 cells, respectively.

Y_2R antagonism of **21 a** was investigated in a fura-2 based Ca^{2+} assay on hY_2R-expressing CHO cells under different conditions: (1) simultaneous incubation of the cells with pNPY and **21 a**; (2) pre-incubation with **21 a** for 20 minutes prior to stimulation with pNPY (Figure 2 a, b). Concentration–response curves (CRCs) of NPY were constructed in the absence and presence of different concentrations of the antagonist, and the data were subjected to Schild analysis.[20]

Simultaneous addition of pNPY and **21 a** led to a parallel rightward shift of the CRCs of pNPY, suggesting competitive antagonism by analogy with previous reports on BIIE 0246.[21,22] Schild regression, constructed from the set of CRCs obtained upon co-application of pNPY with **21 a** (Figure 2 a), revealed a slope of 1.3, which was not significantly different from unity (t-test, α = 0.05). The pA_2 value reflects the affinity of the antagonist; the A_2 value (43 nM) equals the K_d value determined from the study of binding kinetics (Table 2). By contrast, pretreatment of the cells with **21 a** strongly decreased the maximal agonist response in a concentration-dependent manner, indicating insurmountable antagonism against pNPY (Figure 2 b).[22,23] The depression of the maximal response to pNPY by **21 a** was concentration- and time-dependent as shown in Figure 3.

The radioactive form of **21 a**, compound **21 b**, was characterized by saturation and kinetic binding experiments. Saturation experiments with **21 b** using CHO-hY_2R cells afforded a K_d value of 67 nM (Table 3), which was higher than expected from previous flow cytometric binding assays (K_i = 9.9 nM, see **21 a** in Table 1), determined by displacement of fluorescence-labeled pNPY (Dy-635-pNPY). The radioligand showed a low nonspecific binding (Figure 4 a). Scatchard analysis of saturation binding revealed linearity, which is consistent with the presence of a single binding site (Figure 4 b).[24] The maximum number of binding sites (B_{max}) amounted to approximately

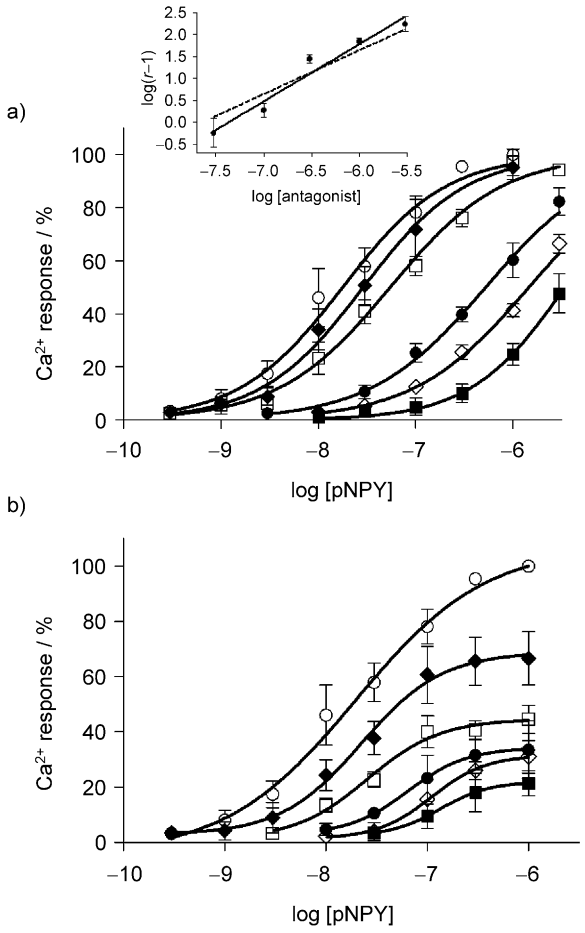

Figure 2. Concentration–response curves (CRCs) of pNPY in the presence of **21 a** obtained from fura-2 assays on CHO-hY_2R cells. a) Simultaneous addition of pNPY and antagonist **21 a** at different concentrations: control (○); **21 a**: 30 nM (◆); 100 nM (□); 300 nM (●), 1000 nM (◇), 3000 nM (■). Inset: Schild regression: log(*r*–1) plotted against the log of antagonist concentration; the concentration ratios *r* ($r = 10^{\Delta pEC50}$) were calculated from the rightward shifts (ΔpEC_{50}) of the CRCs when co-incubated with **21 a** (dashed line: slope = 1; continuous line: slope = 1.31 ± 0.16). $pA_2 = 7.37$; $A_2 = 43$ nM. Completion of the CRCs beyond pNPY concentrations higher than 3 μM was abandoned for economic reasons. b) CRCs of pNPY constructed after pretreatment of the cells with different concentrations of antagonist **21 a** for 20 min: control (○); **21 a**: 30 nM (◆); 100 nM (□); 300 nM (●), 1000 nM (◇), 3000 nM (■). Data represent the mean ± SEM ($n = 3$–8).

175 000 per cell. The results from kinetic studies of **21 b** are presented in Figure 5. Association was almost complete after 30 minutes (Figure 5 a). Dissociation experiments in the presence of pNPY (data not shown), the low-molecular-weight Y_2R antagonist SF-11[6] (data not shown) or BIIE 0246 (Figure 5 b) led to comparable results. After 90 minutes, the residual specific binding of the tritiated compound amounted to approximately 25 %, suggesting in part irreversible binding. However, the equilibrium dissociation constant of **21 b**, calculated from the linearization of the kinetics ($K_d = k_{off}/k_{on} = 43$ nM; Figure 4), was in agreement with the K_d value derived from saturation binding experiments ($K_d = 67$ nM) proving that radioligand **21 b** follows the law of mass action.[24]

Table 3. Y_2R binding and functional characteristics of **21 a**/**21 b**.

k_{off}[a] [min^{-1}]	k_{on}[b] [min^{-1} nM^{-1}]	k_{off}/k_{on}[c] [nM]	K_d[d] [nM]	A_2[e] [nM]
0.030	0.000692	43	67	43

[a] Dissociation rate constant from linear regression. [b] Association rate constant from linear regression. [c] Kinetically derived dissociation constant. [d] Equilibrium dissociation constant determined in saturation binding experiments. [e] Antagonist dissociation constant of **21 a** derived from Schild analysis.

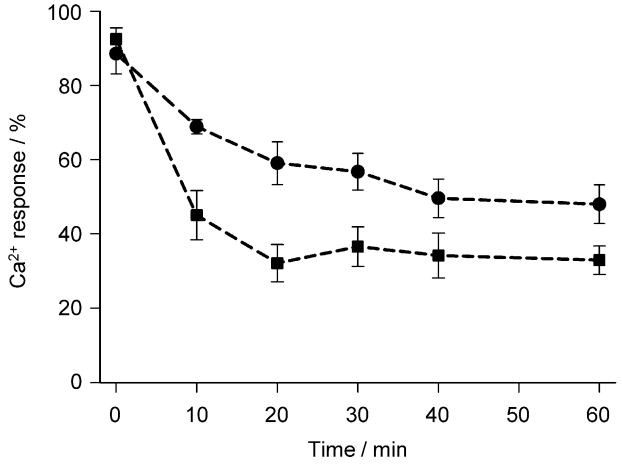

Figure 3. Time course of the pNPY ($c = 300$ nM)-induced Ca^{2+} signal in the presence of antagonist **21 a**. Fura-2 assay on CHO-hY_2R cells performed after pretreatment of the cells with **12 a** (●, 30 nM; ■, 75 nM) for different periods of time.

In contrast to the dissociation experiments, competition binding studies showed that the radioligand was completely displaceable and revealed tremendous discrepancies, when competitors of a different chemical nature were used. In case of nonpeptide Y_2R antagonists, the displacement was monophasic and in the expected concentration range. By contrast, pNPY displaced radioligand **21 b** in a biphasic manner (Figure 6 a). The high-affinity binding site corresponds to a K_i value of 2.0 nM, which is close to the data for pNPY determined by displacement of [^{3}H]propionyl-pNPY ($K_i = 0.4 \pm 0.1$ nM)[16] or Cy5-labeled pNPY ($K_i = 0.8 \pm 0.2$ nM).[16] Displacement of the major portion (80 %) of specifically bound **21 b** required approximately 1000-fold higher concentration of pNPY, corresponding to a K_i value of 1300 nM. The behavior of the nonpeptide antagonist against pNPY was dependent on the order in which labeled ligand and competitor were added and on the duration of the incubation period. When the competition binding experiment was performed in an inverse manner, that is to say by displacing Dy-635-pNPY with **21 a** in a flow cytometric assay (Figure 6 b), the K_i value of **21 a** was comparable with the K_d value of **21 b**.

Recently, a Y_5R-selective radioligand with similar behavior in kinetic and functional experiments was reported as an insurmountable pseudo-irreversible nonpeptide antagonist.[25] Possi-

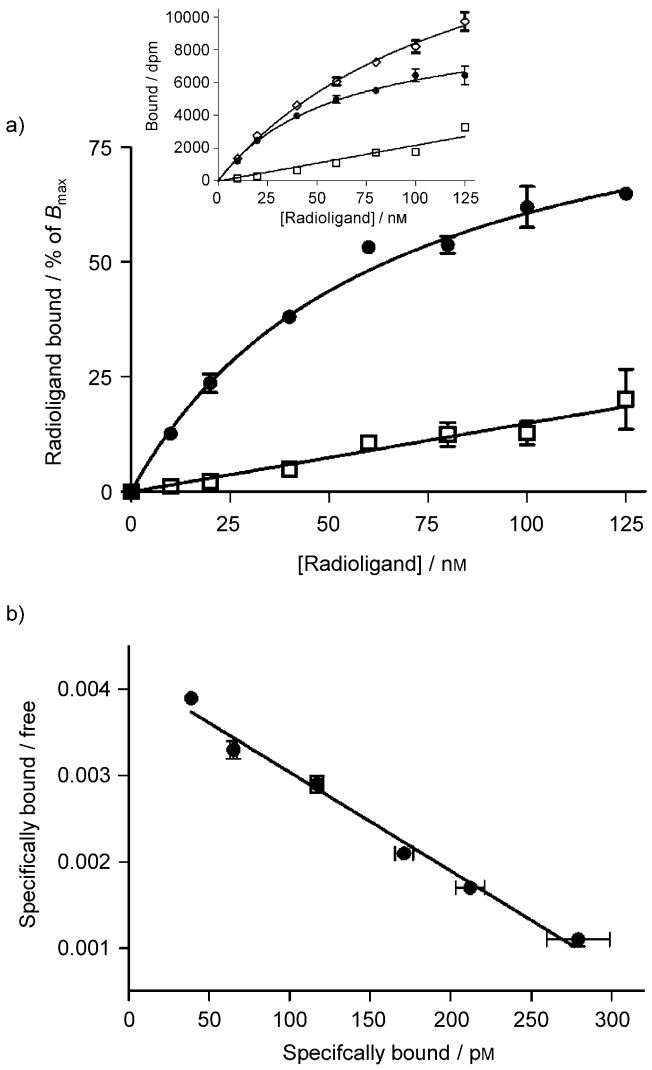

Figure 4. a) Saturation binding of **21 b** at CHO-hY_2R cells. Data represent the mean ± SEM from four independent experiments, performed in triplicate. Specific binding: ●; nonspecific binding: □; $K_{d(sat)} = 67 \pm 14$ nM; Inset: Representative saturation binding curve (dpm), one experiment, performed in triplicate. b) Scatchard plot from data shown in panel a), best fitted by linear regression, $K_d = -1/\text{slope} = 87$ nM.

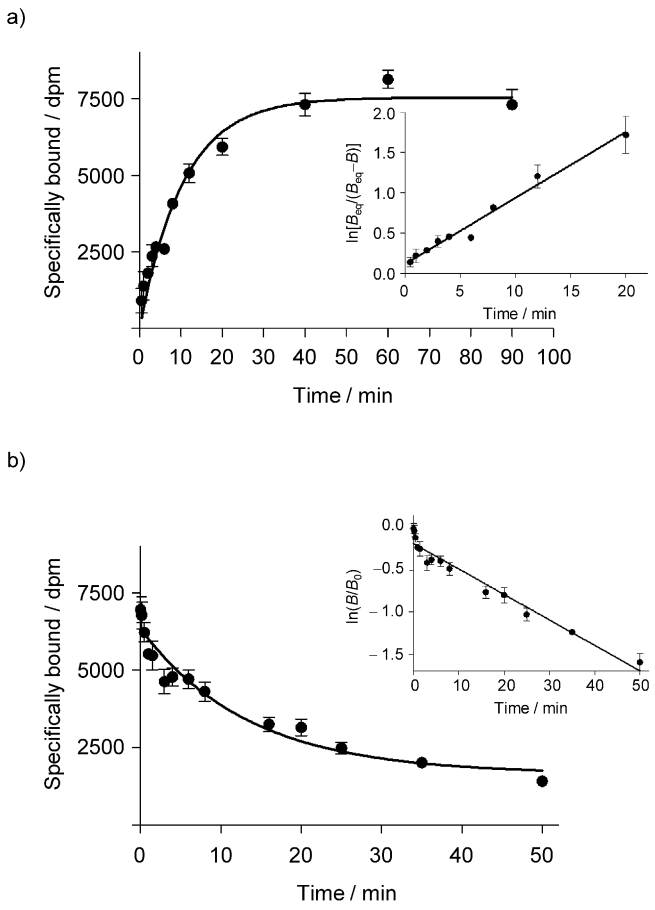

Figure 5. Association and dissociation kinetics of the specific Y_2R binding of **21 b** at CHO-hY_2R cells. a) Radioligand ($c = 75$ nM) association as a function of time. Inset: Linearization $\ln[B_{eq}/(B_{eq}-B)]$ versus time of the association kinetics for the determination of k_{ob}, slope $= k_{ob} = 0.082$ min^{-1}, $k_{on} = (k_{ob} - k_{off})/[L] = 6.92 \times 10^{-4}$ min^{-1} nM^{-1}. b) Radioligand ($c = 75$ nM, pre-incubation for 30 min) dissociation as a function of time, monophasic exponential fit, $t_{1/2} = 9.3$ min, dissociation performed with 100-fold excess of BIIE 0246. Inset: Linearization $\ln(B/B_0)$ versus time of the dissociation kinetic for the determination of $k_{off} = \text{slope} \times (-1) = 0.030$ min^{-1}. Data represent the mean ± SEM ($n = 3$).

ble explanations for such a behavior are a slow rate of dissociation from the receptor,[26] a slow rate of interconversion between inactive and active receptor conformations,[27,28] stabilization of an inactive ligand (antagonist)-specific receptor conformation,[29] or binding to a site distinct from the peptide agonist binding site.[30] The presented data suggest that the Y_2R binding sites of BIIE 0246-derived antagonists and NPY are different or overlap only partially.

Regardless of the special binding characteristics in competition with the peptide, radioligand **21 b** proved to be very useful as a standard ligand in competition binding studies with nonpeptide Y_2R antagonists as shown in Figure 7. The K_d value determined from binding kinetics was applied for the calculation of K_i values by means of the Cheng–Prusoff equation.[31] The binding affinity of BIIE 0246 ($K_i = 17$ nM) is consistent with reported data from competition binding using radiolabeled agonists ($K_i = 24$ nM[32] and 36 nM[21]). Furthermore, the dissociation constants of the other investigated compounds are in good agreement with data from flow cytometric binding studies (Table 1). The K_i value of **21 a** (36 nM), determined by competition binding experiments with the labeled analogue **21 b**, corresponds very well to the K_d value of compound **21 b** (43 nM).

In summary, the guanidine–acylguanidine bioisosteric approach was applied to the preparation of a tritiated Y_2R-selective radioligand starting from the highly potent argininamide-type Y_2R antagonist BIIE 0246. Acylation of the amine precursor, N^G-[5-(2-aminoethylamino)-5-oxopentanoyl]-substituted BIIE 0246 (**11**), with succinimidyl [2,3-^{3}H]propionate ($a_s = 80.7$ Ci mmol^{-1}) afforded desired radioligand **21 b**. Nonpeptidic radioligand **21 b** ([^{3}H]UR-PLN196) is superior to Y_2R-addressing radiolabeled native peptides due to NPY-receptor-subtype selectivity, resistance against cleavage by peptidases, long-term stability, mode of action (antagonist vs agonist), and costs of

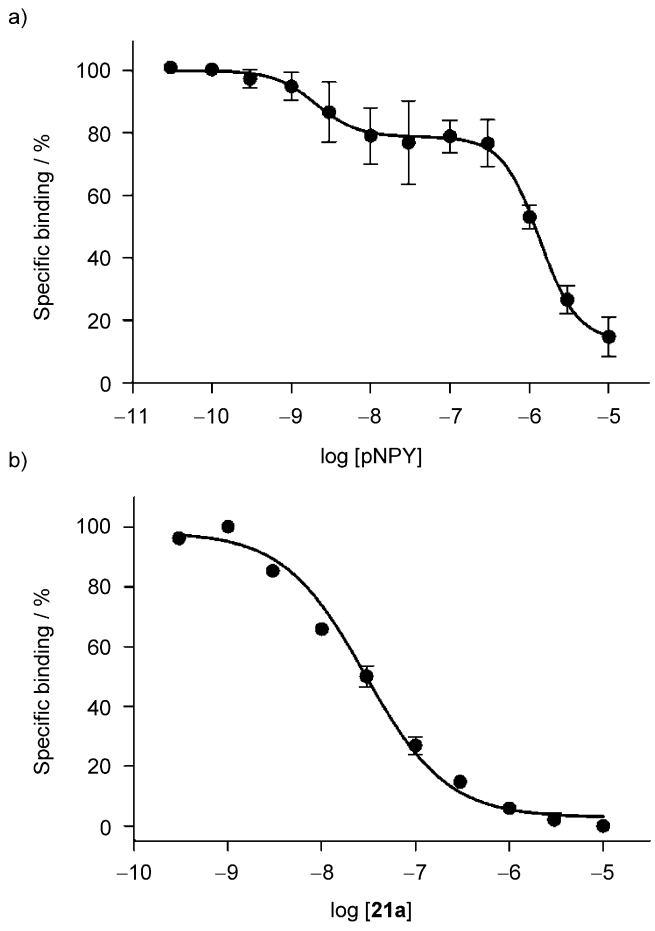

Figure 6. a) Displacement of tritiated Y_2R antagonist **21 b** ($c = 75$ nM) by the agonist pNPY. $K_{i1} = 2.0 \pm 1.1$ nM, $K_{i2} = 1300 \pm 700$ nM. b) Flow cytometric competition binding. Displacement of Dy-635-pNPY ($c = 5$ nM, $K_d = 5.2$ nM) by **21 a**, the "cold form" of the radioligand, $K_i = 9.9 \pm 3.0$ nM. The binding was determined after an incubation period of 120 min on CHO cells stably expressing the human Y_2R. Data represent the mean ± SEM ($n = 3$).

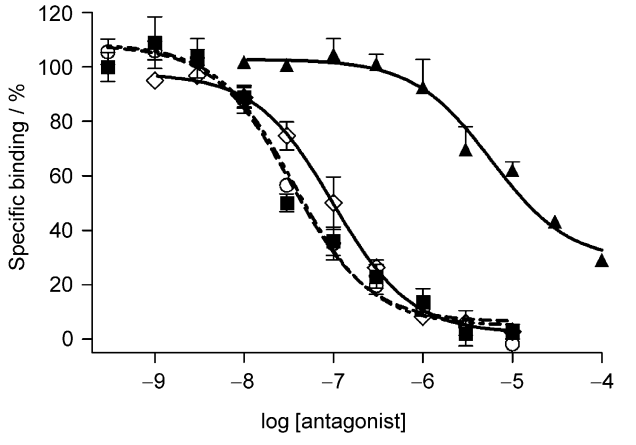

Figure 7. Displacement of the radioligand **21 b** ($c = 75$ nM, $K_d = 43$ nM) by argininamide-type Y_2R antagonists BIIE 0246 (○, $K_i = 17 \pm 2.6$ nM), **16** (■, $K_i = 16 \pm 3.0$ nM), **21 a** (◇, $K_i = 47 \pm 7.3$ nM) and the low-molecular-weight Y_2R-selective antagonist SF-11 (▲, $K_i = 2750 \pm 710$ nM). The assay was performed on CHO cells stably expressing the Y_2R with an incubation period of 30 min. Data represent the mean ± SEM ($n = 2$–3).

preparation. [^{3}H]UR-PLN196 can be used for the detection and quantification of Y_2R binding sites. Detailed investigations in binding experiments (with **21 b**) and functional assays (with **21 a**) revealed insurmountable antagonism versus pNPY and pseudoirreversible binding at the Y_2R. Moreover, the tritiated compound was successfully applied as a standard ligand in competition binding experiments with several Y_2R antagonists. In conclusion, the prepared radioligand (**21 b**) is a valuable pharmacological tool for the detection of Y_2R, for investigations on ligand binding modes, and for the characterization of nonpeptidic Y_2 receptor antagonists.

Experimental Section

Chemicals and solvents were purchased from commercial suppliers and used without further purification. Porcine NPY (pNPY) was kindly provided by Prof. Dr. Chiara Cabrele (Paris-Lodron University, Salzburg, Austria). SF-11 was purchased from Tocris Bioscience (Bristol, UK). All solvents were of analytical grade or distilled prior to use. Succinimidyl [2,3-^{3}H]propionate was from Hartmann Analytic (Braunschweig, Germany) and provided as a solution in hexane/EtOAC (9:1 *v/v*) ($a_s = 3.07$ TBq mmol^{-1} = 83 Ci mmol^{-1}; 185 MBq/2.5 mL).

Analytical and preparative HPLC were performed on a Waters system (two pumps 510, pump control module, 486 UV detector, Packard Radiomatic Flow-1 beta series A-500 detector, liquid scintillator (Rotiszint eco plus, Carl Roth GmbH & Co. KG, Karlsruhe, Germany) flow rate: 4 mL min^{-1}) using a Synergi C-18 column (250 × 4.6 mm, 5 μm). See the Supporting Information for a detailed description of the preparation and analytical characterization of compounds **1**–**20**, **21 a**, **22**–**30**, **32**–**34**, purity (determined by HPLC) of **11**–**20**, **21 a**, **22**–**30** and **32**–**34**, long-term stability **21 b** controlled by HPLC, and pharmacological methods.

(2*S*)-*N*-[2-(3,5-Dioxo-1,2-diphenyl-1,2,4-triazolidin-4-yl)ethyl]-*N*$^{\alpha}$-[2-(1-{2-oxo-2-[4-(6-oxo-6,11-dihydro-5*H*-dibenzo[*b*,*e*]azepin-11-yl)piperazin-1-yl]ethyl}cyclopentyl)acetyl]-*N*$^{\omega}$-[4-(2-[2,3-^{3}H]-propanoylaminoethyl)aminocarbonylbutanoyl]argininamide (21 b): Compound **11** (1.23 mg, 0.964 μmol) was dissolved in anhydrous CH_3CN (140 μL) yielding a concentration of 6.9 mM, and NEt_3 was diluted in CH_3CN to a concentration of 2.7 μL NEt_3/100 μL. Compound **11** (6.9 mM in CH_3CN, 50 μL, 0.344 μmol) and NEt_3 (10 μL of the above described solution in CH_3CN, 1.928 μmol) were added to succinimidyl [2,3-^{3}H]propionate (4.22 μg, 0.0241 μmol) in 1 mL hexane/EtOAc (9:1 *v/v*) in a 1.5 mL Eppendorf reaction vessel (screw top). The solvent was removed in a vacuum concentrator (40 °C) over a period of 20 min and additional **11** (6.9 mM in CH_3CN, 90 μL, 0.620 μmol) was added. Again, the solvent was removed in a vacuum concentrator (40 °C) over a period of 40 min. After addition of 100 μL of CH_3CN, the reaction mixture was vigorously blended (vortexer) for 1 min, briefly centrifuged and stirred with a magnetic microstirrer at RT overnight.

For HPLC analysis, 0.5 μL of the reaction mixture (reaction control) were diluted (1:200) with CH_3CN/0.05% aq. TFA (30/70, 97.5 μL) and spiked with "cold" radioligand **21 a** (1 mM in CH_3CN, 2 μL) to a total volume of 100 μL. This solution was completely injected into the HPLC system and analyzed by means of UV and radiometric detection. Eluent: CH_3CN + 0.05% aq. TFA (A) and 0.05% aq. TFA (B), gradient: 0 to 25 min: A/B 30/70 to 55/45, 25 to 27 min: 55/45 to 95/5, 27 to 35 min: 95/5. Afterwards, the reaction was stopped with 10% aq. TFA (2.9 μL, corresponds to ≈160 eq of

TFA), and the reaction mixture was purified with analytical HPLC. Therefore, the reaction mixture was diluted with 0.1% aq. TFA (350 μL), and the product was isolated (three injections) using the conditions specified for the reaction control. In this instance, radiometric detection was not performed. The product was eluted at 18.8 to 19.3 min and collected in a 1.5 mL Eppendorf reaction vessel (screw top), which was put into the vacuum concentrator between injections. The combined product fractions were evaporated to dryness in a vacuum concentrator, the residue was dissolved in 300 μL of EtOH containing TFA (100 μM) and transferred to a clean 3 mL Amersham glass vial together with the washings (2×100 μL).

Quantification: A five-point calibration was performed with **21a** (0.25, 0.5, 1.0, 1.5 and 3.0 μM; injection volume: 100 μL). Eluent: CH_3CN + 0.05% aq. TFA (A) and 0.05% aq. TFA (B), gradient: 0 to 20 min: A/B 30/70 to 60/40, 20 to 20 min: 60/40 to 95/5, 22 to 30 min: 95/5 (t_R = 15.72 min). The solutions for injection were prepared in CH_3CN/0.05% aq. TFA (20/80) less than 5 min prior to injection. All standard solutions were prepared from a 40 μM solution of **21a** (in CH_3CN/0.05% aq. TFA 20/80), which was freshly made from a 1 mM stock solution of **21a** in CH_3CN. Two aliquots (2.0 μL) of the ethanolic solution (total volume: 500 μL) of the product were diluted with 100 μL of CH_3CN/0.05% aq. TFA (20/80), and 100 μL were analyzed by HPLC. Whereas one sample was only used for quantification of the product by UV detection, the second sample was additionally monitored radiometrically to determine radiochemical purity. The molarity of the ethanolic solution of **21b** was calculated from the mean of the peak areas, and the linear calibration curve was obtained from the peak areas of the standards. Yield: 9.1 μg (7.41 nmol, 31%).

Determination of the specific activity: An aliquot (1.5 μL) of the ethanolic solution were diluted with 448.5 μL of a mixture of CH_3CN and water (50/50) in duplicate, and 9 μL of the 1:300 dilutions were counted in Rotiszint eco plus (3 mL). Specific activity (a_s): 2.99 TBq mmol^{-1} (80.7 Ci mmol^{-1}). The activity concentration (a_v) was adjusted to 3.59 MBq mL^{-1} (0.097 mCi mL^{-1}) by addition of EtOH (1685 μL) containing TFA (100 μM) to the residual solution yielding a molarity of 1.20 μM. The radioligand **21b** was stored at −20 °C.

Acknowledgements

The authors thank Elvira Schreiber and Brigitte Wenzl for expert technical assistance. This work was supported by the Deutsche Forschungsgemeinschaft Graduate Training Program (Graduiertenkolleg) GRK 760.

Keywords: acylguanidines · bioisosterism · neuropeptide Y · radiochemistry · radioligands

[1] S. P. Brothers, C. Wahlestedt, *EMBO Mol. Med.* **2010**, *2*, 429 – 439.
[2] E. Yulyaningsih, L. Zhang, H. Herzog, A. Sainsbury, *Br. J. Pharmacol.* **2011**, *163*, 1170 – 1202.
[3] H. Doods, W. Gaida, H. A. Wieland, H. Dollinger, G. Schnorrenberg, F. Esser, W. Engel, W. Eberlein, K. Rudolf, *Eur. J. Pharmacol.* **1999**, *384*, R3 – 5.
[4] J. R. Shoblock, N. Welty, D. Nepomuceno, B. Lord, L. Aluisio, I. Fraser, S. T. Motley, S. W. Sutton, K. Morton, R. Galici, J. R. Atack, L. Dvorak, D. M. Swanson, N. I. Carruthers, C. Dvorak, T. W. Lovenberg, P. Bonaventure, *Psychopharmacology* **2010**, *208*, 265 – 277.
[5] P. Bonaventure, D. Nepomuceno, C. Mazur, B. Lord, D. A. Rudolph, J. A. Jablonowski, N. I. Carruthers, T. W. Lovenberg, *J. Pharmacol. Exp. Ther.* **2004**, *308*, 1130 – 1137.
[6] S. P. Brothers, S. A. Saldanha, T. P. Spicer, M. Cameron, B. A. Mercer, P. Chase, P. McDonald, C. Wahlestedt, P. S. Hodder, *Mol. Pharmacol.* **2010**, *77*, 46 – 57.
[7] G. K. Mittapalli, D. Vellucci, J. Yang, M. Toussaint, S. P. Brothers, C. Wahlestedt, E. Roberts, *Bioorg. Med. Chem. Lett.* **2012**, *22*, 3916 – 3920.
[8] J. Nozulak, D. Oser, J. Daehler, D. Orain, S. Cotesta, D. Uzunov, *XXIInd International Symposium on Medicinal Chemistry*, (Berlin, Germany, Sept 2 – 6, 2012), Book of Abstracts, *ChemMedChem*, Wiley-VCH, Weinheim, **2012**, pp. 306 – 307, abstract: P475.
[9] R. S. Chang, V. J. Lotti, T. B. Chen, *Biochem. Biophys. Res. Commun.* **1988**, *151*, 1213 – 1219.
[10] P. S. Widdowson, A. E. Halaris, *J. Neurochem.* **1990**, *55*, 956 – 962.
[11] J. C. Martel, A. Fournier, S. St. Pierre, R. Quirion, *Neuroscience* **1990**, *36*, 255 – 283.
[12] Y. Dumont, A. Fournier, S. St-Pierre, R. Quirion, *J. Pharmacol. Exp. Ther.* **1995**, *272*, 673 – 680.
[13] Y. Dumont, A. Fournier, S. St-Pierre, R. Quiron, *Synapse* **1996**, *22*, 139 – 158.
[14] N. Pluym, A. Brennauer, M. Keller, R. Ziemek, N. Pop, G. Bernhardt, A. Buschauer, *ChemMedChem* **2011**, *6*, 1727 – 1738.
[15] M. Keller, N. Pop, C. Hutzler, A. G. Beck-Sickinger, G. Bernhardt, A. Buschauer, *J. Med. Chem.* **2008**, *51*, 8168 – 8172.
[16] R. Ziemek, A. Brennauer, E. Schneider, C. Cabrele, A. G. Beck-Sickinger, G. Bernhardt, A. Buschauer, *Eur. J. Pharmacol.* **2006**, *551*, 10 – 18.
[17] E. Schneider, M. Mayer, R. Ziemek, L. Li, C. Hutzler, G. Bernhardt, A. Buschauer, *ChemBioChem* **2006**, *7*, 1400 – 1409.
[18] M. Müller, S. Knieps, K. Gessele, S. Dove, G. Bernhardt, A. Buschauer, *Arch. Pharm.* **1997**, *330*, 333 – 342.
[19] R. Ziemek, E. Schneider, A. Kraus, C. Cabrele, A. G. Beck-Sickinger, G. Bernhardt, A. Buschauer, *J. Recept. Signal Transduction Res.* **2007**, *27*, 217 – 233.
[20] O. Arunlakshana, H. O. Schild, *Br. J. Pharmacol. Chemother.* **1959**, *14*, 48 – 58.
[21] F. M. Dautzenberg, *Biochem. Pharmacol.* **2005**, *69*, 1493 – 1499.
[22] F. M. Dautzenberg, S. Neysari, *Pharmacology* **2005**, *75*, 21 – 29.
[23] G. Vauquelin, I. Van Liefde, B. B. Birzbier, P. M. Vanderheyden, *Fundam. Clin. Pharmacol.* **2002**, *16*, 263 – 272.
[24] S. Lazareno, *J. Recept. Signal Transduction Res.* **2001**, *21*, 139 – 165.
[25] D. Mullins, N. Adham, D. Hesk, Y. Wu, J. Kelly, Y. Huang, M. Guzzi, X. Zhang, S. McCombie, A. Stamford, E. Parker, *Eur. J. Pharmacol.* **2008**, *601*, 1 – 7.
[26] S. Meini, R. Patacchini, A. Lecci, L. Quartara, C. A. Maggi, *Eur. J. Pharmacol.* **2000**, *409*, 185 – 194.
[27] F. L. Fierens, P. M. Vanderheyden, J. P. De Backer, G. Vauquelin, *Eur. J. Pharmacol.* **1999**, *372*, 199 – 206.
[28] G. Vauquelin, P. Morsing, F. L. Fierens, J. P. De Backer, P. M. Vanderheyden, *Biochem. Pharmacol.* **2001**, *61*, 277 – 284.
[29] R. Seifert, E. H. Schneider, S. Dove, I. Brunskole, D. Neumann, A. Strasser, A. Buschauer, *Mol. Pharmacol.* **2011**, *79*, 631 – 638.
[30] S. Lazareno, N. J. Birdsall, *Mol. Pharmacol.* **1995**, *48*, 362 – 378.
[31] Y.-C. Cheng, W. H. Prusoff, *Biochem. Pharmacol.* **1973**, *22*, 3099 – 3108.
[32] R. Ziemek, Ph.D. thesis, University of Regensburg (Regensburg, Germany), **2006**.

Received: December 10, 2012
Published online on January 29, 2013